

Facile synthesis of morphology- and size-controllable polythiophene/gold composites in aqueous medium

Quanhui Guo · Shuangshuang Zou · Juan Li ·
Dongfeng Li · Hexian Jiao · Jiahua Shi

Received: 15 May 2014 / Accepted: 10 October 2014 / Published online: 17 October 2014
© Springer Science+Business Media Dordrecht 2014

Abstract Polythiophene (PTh) nanomaterials and polythiophene/gold (PTh-Au) composites were successfully fabricated using chloroaurate acid (HAuCl_4) as an oxidant in aqueous medium without using any templates or structure-directing agents. With increasing thiophene (Th) concentration from 0.5 to 50 mM at a fixed molar ratio of thiophene and HAuCl_4 of 3:1, Au@PTh core-shell nanoparticles (~ 36 nm in diameter) and fibers, AuNPs-modified PTh nanospheres (~ 270 nm in diameter), flower-like gold microparticles, and gold microspheres were obtained. At a fixed thiophene concentration of 5.0 or 50 mM, the molar ratio of thiophene/ HAuCl_4 also affected the morphology and size of PTh-Au composites. The morphology of obtained nanostructures was determined by scanning electron microscope and transmission electron microscope. Furthermore, characterization experiments including FT-IR, UV-Vis spectrometry, energy-dispersive X-ray spectroscopy, and selected-area electron diffraction were utilized to investigate the chemical and

electronic structures of PTh nanostructures and PTh-Au composites. The photoluminescent (PL) properties of PTh-Au composites have also been investigated to clarify the effectiveness of the morphology and composition of composites on the PL emission peaks. In addition, the formation mechanism of PTh nanostructures and PTh-Au composites is also proposed.

Keywords Polythiophene · Gold nanoparticle · Composite · Nanosphere · Conducting polymers · Nanofiber

Introduction

Polythiophene (PTh), an environmentally and thermally stable conjugated polymer material (McCullough 1999), has received a great deal of attention because of its potential applications in electrical conductors, antistatic coatings, sensors, photovoltaic devices, polymer light-emitting diodes, solar cells, and transistors (Skotheim et al. 1998; Kim et al. 2006, 2014; Pandey et al. 2008; Kline et al. 2006; Ho et al. 2008; Mwaura et al. 2006; Andersson et al. 1995; Zou et al. 2007; Gevorgyan and Krebs 2008; Thompson and Fréchet 2008; Gunes et al. 2007; Bao et al. 1996). However, the extremely poor processability of the unsubstituted PTh limits its further extensive application. Although elaborate efforts have been taken to incorporate various substituent groups such as alkyl, alkoxy, amine, sulfonic, and carboxylic acids to

Electronic supplementary material The online version of this article (doi:10.1007/s11051-014-2702-x) contains supplementary material, which is available to authorized users.

Q. Guo · S. Zou · J. Li · D. Li · H. Jiao · J. Shi (✉)
Engineering Laboratory for Flame Retardant and
Functional Materials of Henan Province, College of
Chemistry and Chemical Engineering, Institute of Fine
Chemical and Engineering, Henan University,
Kaifeng 475004, China
e-mail: sjiahua@henu.edu.cn

improve the solubility of thiophene (McCullough et al. 1993; Sheina et al. 2005; Ogawa et al. 2005; Bao and Lovinger 1999; Chayer et al. 1997), these synthetic procedures are quite complex and expensive.

One of the alternatives to improve the processability of the unsubstituted PTh is the preparation of nanostructured PTh by heterogeneous oxidative polymerization. Tran et al. have pointed out that only agglomerated structures of PTh will be obtained with the traditional oxidative polymerization method (Tran et al. 2008). Up to now, template synthesis has been the main technique for preparing nanoscale PTh materials such as nanotubes or nanowires (Fu et al. 2001; Li et al. 2003). In addition, surfactant method has also been applied to fabricate PTh nanostructures in traditional oxidative polymerization in organic solvents such as chloroform and acetonitrile with ferric chloride (FeCl_3) as the oxidant (Gök et al. 2007; Li et al. 2009a, b). Although water is an environmentally friendly medium, oxidative polymerization of unsubstituted thiophene monomers in aqueous medium has been reported in only a few cases due to the high oxidation potential and poor solubility of thiophene in water (Alkan et al. 2003). Recently, Kim and co-workers first reported the fabrication of PTh nanoparticles via oxidative polymerization of unsubstituted thiophene monomers in aqueous medium by using $\text{FeCl}_3/\text{H}_2\text{O}_2$ (catalyst/oxidant) and sodium dodecyl sulfate (SDS, surfactant) combination system (Lee et al. 2008a, b; Lee et al. 2010a, b). Similarly, Wang et al. also obtained PTh nanoparticles by copper (II)-catalyzed oxidative emulsion polymerization with a series of copper (II) salts as oxidants in the presence of anionic surfactant SDS and H_2O_2 (Wang et al. 2010).

Until now, PTh nanomaterials have been fabricated either within templates or with structure-directing agents. Moreover, other oxidants besides the conventional oxidant FeCl_3 should be explored to fabricate different nanostructured PTh. Recently, chloroaurate acid (HAuCl_4) has been used as an oxidant to study the polymerization of thiophene and prepare PTh–Au composites. Chattopadhyay et al. first reported one-pot synthesis of polythiophene–gold nanoparticles (AuNPs) composites and then developed a reversible pH sensor and a new method for bacterial quantification based on the fluorescence properties of the PTh–AuNPs composites (Panda and Chattopadhyay 2007; Panda et al. 2008). The ‘superquenching’ property of AuNPs to water-soluble fluorescent polythiophene

derivatives was also utilized to detect aspartic acid and glutamic acid (Guan et al. 2008). However, the visible photoluminescence of ultrathin poly(3-hexylthiophene) films could increase extensively by the incorporation of about 5-nm AuNPs into the matrix (Nicholson et al. 2005). Kim and colleagues prepared ‘raspberry-like’ PTh–gold nanoaggregates which possess enhanced photoluminescent intensities because the surface plasmon energy of AuNPs matches with the emitted photon energy of PTh which results in the resonance introducing energy transfer (Jung et al. 2010). Very recently, Suzuki et al. investigated the magnetic and electrical transport properties of regio-regular poly(3-hexylthiophene)-capped AuNPs doped with iodine (Suzuki et al. 2011). AuNPs-embedded PTh vesicles were also controllably prepared from thiophene and AuNPs in aqueous solution in the presence of H_2O_2 , SDS, and a catalytic amount of FeCl_3 (Sun et al. 2011). So far, many efforts have been devoted to the design and synthesis of various PTh–AuNPs nanocomposites to enhance the optical and electronic properties of polythiophene.

In the present study, one of our aims is to synthesize PTh nanomaterials using HAuCl_4 as the oxidant in aqueous medium without using any templates or structure-directing agents, and the other aim is to fabricate various PTh–Au composites with different morphologies and properties. The synthesis of PTh was carried out under different reaction conditions, i.e., varying thiophene concentrations and molar ratios of thiophene/ HAuCl_4 . The influence of synthetic conditions on the specific morphology and size of PTh–Au composites was also investigated.

Experimental details

Materials

Thiophene monomer was procured from Sigma–Aldrich and used after distillation under reduced pressure. $\text{HAuCl}_4 \cdot 3\text{H}_2\text{O}$ purchased from Alfa Aesar was dissolved in water to make stock solutions of 10 mM and 100 mM.

Synthesis of PTh–Au composites

The synthesis of PTh–Au composites is as follows: Aqueous thiophene solutions of varying concentrations

were prepared by sonicating the required amount of thiophene in 10.0 mL distilled water at room temperature. Subsequently, requisite amounts of HAuCl_4 were added to obtain various molar ratios of thiophene to HAuCl_4 . The reaction mixture was sonicated for 5 min and left overnight at room temperature, without stirring. After 24 h, the dark precipitate was separated via centrifugation at a speed of 6,000 rpm and purified with ethanol and water.

Characterization and instrumentation

The morphologies of the samples were investigated using a JEOL JSM-6701F field emission scanning electron microscope (FE-SEM) and a JEOL JEM 3010F transmission electron microscope (TEM) at 300 kV accelerating voltage. During the SEM experiments, Synchronous Energy-Dispersive X-ray (EDX) analysis was conducted using a LINK ISIS300 instrument. X-ray diffraction patterns were taken with a Bruker AXS D5005 Advance XRD instrument using $\text{CuK}\alpha$ irradiation. Fourier transform infrared (FT-IR) spectra were recorded on a Perkin-Elmer Spectrum 2000 IR spectrometer in the range of 400–4,000 cm^{-1} . The absorption spectra of the samples in ethanol were measured with an UV-Vis spectrophotometer (UV-1700PC, Shimadzu). Photoluminescence spectra were performed on a FL spectrophotometer (F-7000 Hitachi).

Results and discussion

Morphology of PTh–Au composites

The oxidation polymerization of thiophene was carried out using HAuCl_4 as the oxidant by simultaneous reduction of HAuCl_4 to gold nanostructures and polymerization of thiophene in aqueous medium at room temperature. To study the effect of monomer concentration on the morphology of PTh–Au composites, a series of oxidative polymerization experiments were first carried out with different monomer concentrations at the theoretical molar ratio of thiophene and HAuCl_4 of 3:1. The morphology and size of PTh–Au composite powder were observed using SEM. At an extremely low thiophene concentration of 0.5 mM, nanoparticles with an average diameter of approximately 36 nm were obtained (Fig. 1a). When

the concentration of thiophene increases to 1.0 mM, these Au@PTh core–shell nanoparticles tend to merge together and form short fiber-like nanostructures (Fig. 1b). As the thiophene concentration gradually increases to 5 and 10 mM, one-dimensional fibers with various sizes were easily observed in Fig. 1c, d. It is evident that the diameters of one-dimensional fibers increase with increasing monomer concentration from 5 and 10 mM. As the monomer concentration further increases to 50 mM, the morphological transition from one-dimensional fibers to nanospheres and flower-like microparticles can be observed in Fig. 1e. Synchronous EDX analysis confirmed that the flower-like microparticles were made of gold (data not shown). As illustrated in a high-magnification SEM image (the inset in Fig. 1e), the flower-like microparticles comprised many gold nanosheets with the thicknesses of ~ 30 –60 nm. At a high thiophene concentration of 100 mM, irregular microspheres were generated besides nanospheres as shown in Fig. 1f.

The morphology and inner structure of PTh–Au composite powder were further checked by TEM, as shown in Fig. 2. These nanoparticles prepared at 0.5 mM of thiophene should be Au@PTh core–shell nanoparticles which are AuNPs capped with a thin layer of polythiophene. This was confirmed by TEM shown in Fig. 2a, e. A typical TEM image of a single nanofiber at higher magnification is shown in Fig. 2b, f, from which it can be seen that the one-dimensional fiber has a coaxial cable structure composed of many AuNPs core and PTh shell. AuNPs-modified PTh nanospheres with an average diameter of around 270 nm were obtained with small gold nanoparticles incorporated at the periphery of PTh nanospheres, which was further confirmed by TEM image (Fig. 2c, g). The full higher resolution TEM images (Fig. 2e–h) were shown as supplementary material (Fig. S1). The typical selected-area electron diffraction (SAED) pattern of PTh–Au composite powder was obtained by directing the electron beam perpendicular to the samples deposited on the TEM grid. Figure 2i–k shows the corresponding SAED pattern of Au@PTh core–shell nanoparticles, Au@PTh nanofibers, and gold nanoparticles, respectively. The characteristic rings in the polycrystalline diffraction pattern from inner to outer can be indexed to (111), (200), (220), and (311) crystalline facets of face-centered cubic (fcc) lattice gold phase (Guo et al. 2006).

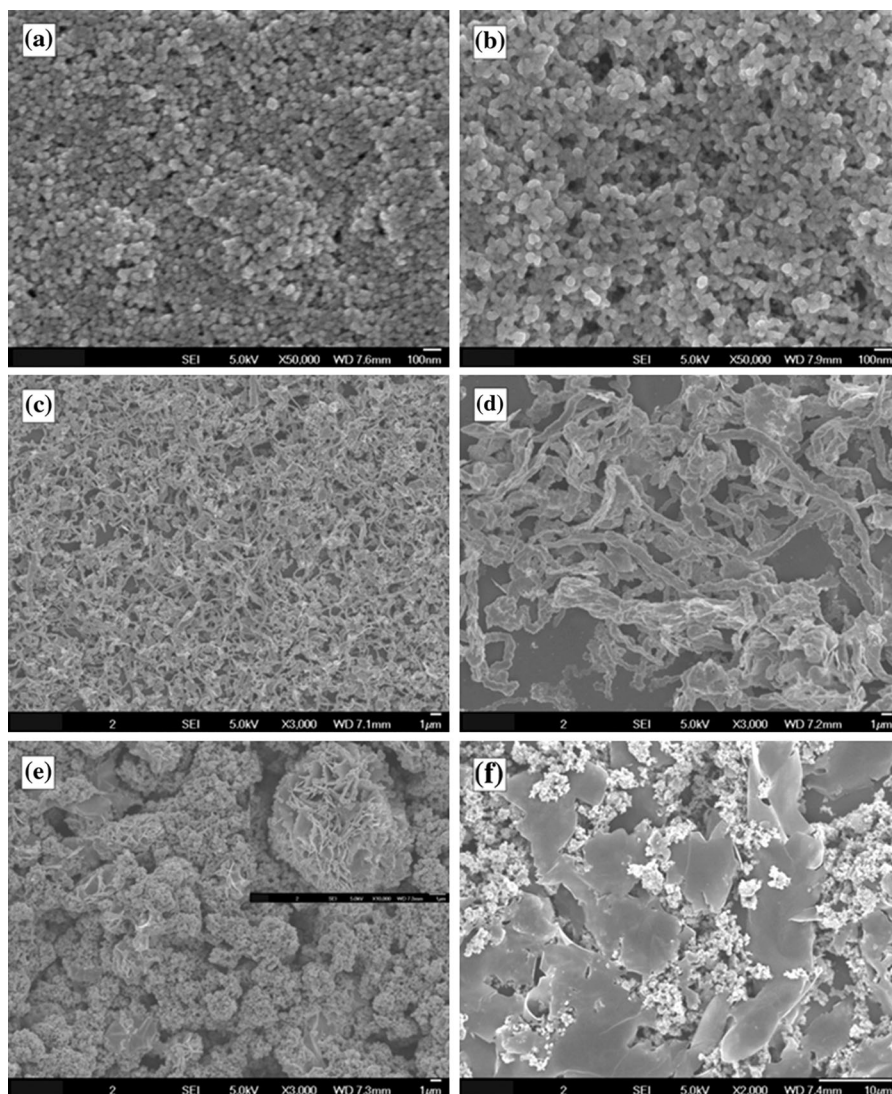


Fig. 1 SEM images of PTh–Au composite powder prepared with various concentrations of thiophene: **a** 0.5 mM, **b** 1.0 mM, **c** 5.0 mM, **d** 10 mM, **e** 50 mM, **f** 100 mM. Other reaction conditions: [Thiophene]/[HAuCl₄] = 3:1, 25 °C, *t* = 24 h

The microsheets synthesized at high thiophene concentration were further observed using TEM. We found that the microsHEET was a gold microsHEET capped with a thin layer of polythiophene (Fig. 2d, h). Figure 2h shows a typical HRTEM image of a gold microsHEET. The well-resolved interference fringe patterns attest to the single crystallinity of this gold sheet. The fringes with a spacing of 0.248 nm could be ascribed to $1/3\{422\}$ lattice spacing of the fcc gold crystal (Bai et al. 2008). The single-crystalline nature of the gold microsHEET was further confirmed by their electron diffraction patterns by focusing the electron beams perpendicular to the basal

plane of a single gold microsHEET (Fig 2i). The hexagonal symmetry of the diffracted spots suggests that the gold microsHEET is a single crystal structure with highly oriented growth direction along the Au (111) plane. Three sets of spots can be identified based on *d*-spacing. The spots (triangle) could be indexed to the $\{220\}$ reflection of fcc gold, the outer spots (square) could be assigned to the allowed $\{422\}$ Bragg reflection, and the inner spots (circle) are believed to originate from the forbidden $1/3\{422\}$ reflection.

The X-ray diffraction (XRD) patterns of the resulting products obtained at different concentrations of

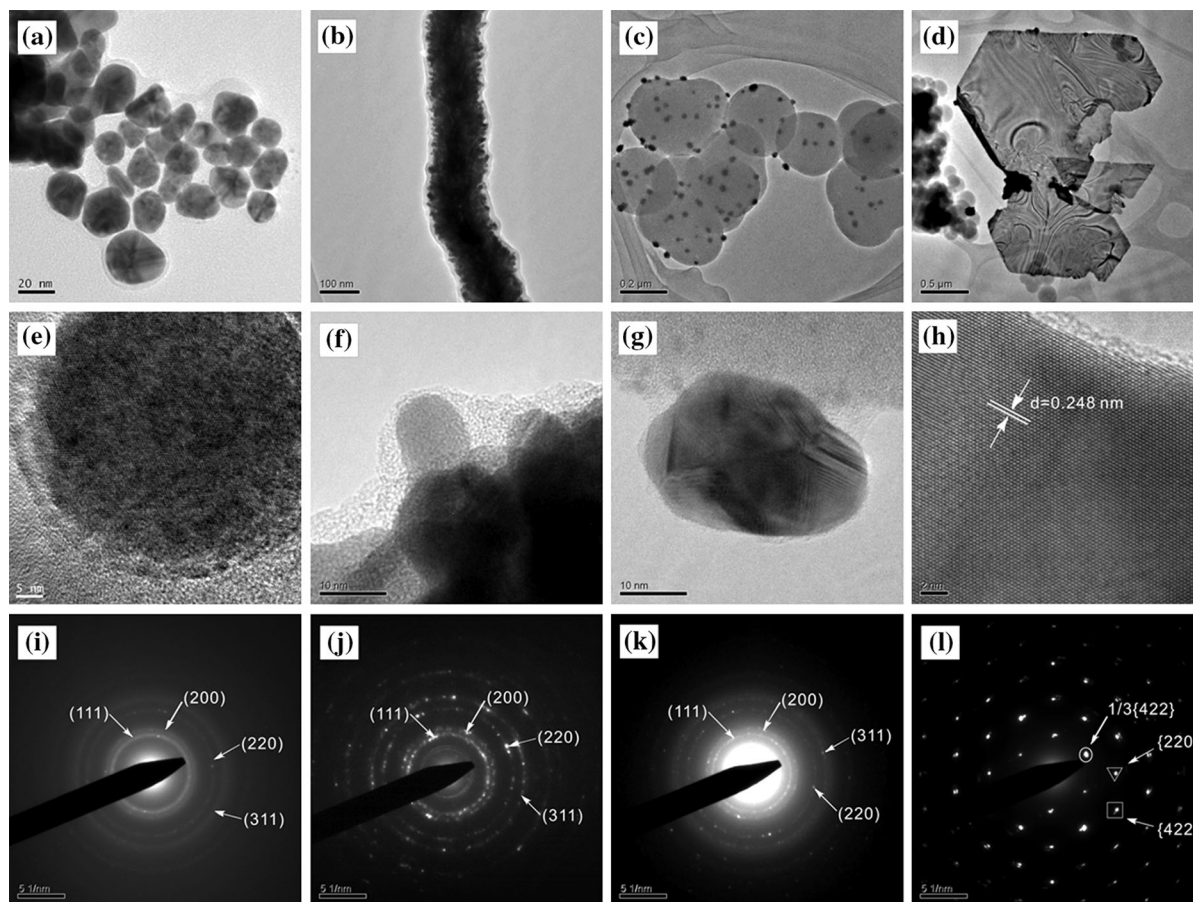


Fig. 2 TEM images (a–d), the corresponding HRTEM images (e–h) and selected-area electron diffraction (SAED) patterns (i–l) of PTh–Au composite powder prepared using 0.5, 5.0, 50, and

100 of thiophene, respectively. Other reaction conditions: [Thiophene]/[HAuCl₄] = 3:1, 25 °C, *t* = 24 h

thiophene are shown in the supporting information (Fig. S2). There are four main peaks at 38, 44, 65, and 78° in the XRD patterns of the resulting products, which correspond to (111), (200), (220), and (311) Bragg reflections of gold, respectively.

We also observed that the molar ratio of thiophene/HAuCl₄ affected the morphology and size of PTh–Au composites. To explore the intrinsic formation mechanism of one-dimensional Au@PTh fibers and AuNPs-modified PTh nanospheres, we conducted a series of experiments by varying the molar ratio of thiophene/HAuCl₄ at a fixed thiophene concentration of 5.0 or 50 mM.

Figure 3 shows the effect of the molar ratio of thiophene/HAuCl₄ on the morphology of products when thiophene concentration was 5.0 mM. When the molar ratio of thiophene/HAuCl₄ was 1:1, 2:1, and 3:1,

respectively, one-dimensional Au@PTh fibers were still produced. With increasing molar ratio of thiophene/HAuCl₄, the average diameters of the fibers decreased accordingly. The reduced amount of HAuCl₄ could result in reduced AuNPs, and the Au@PTh fibers were generated by growing AuNPs as core and a thin PTh layer as shell (Mallick et al. 2007). However, when the molar ratio of thiophene/HAuCl₄ increased to 5:1 and 10:1, the formation of fibers is diminished while agglomerate formation dominates.

When the thiophene concentration was increased to 50 mM, a morphological transition from nanocables to nanospheres was observed. The effect of varying molar ratio of thiophene/HAuCl₄ on PTh nanospheres has also been investigated when the thiophene concentration is 50 mM (as shown in Fig. 4). At a thiophene/HAuCl₄ molar ratio of 5:1 and 3:1, respectively,

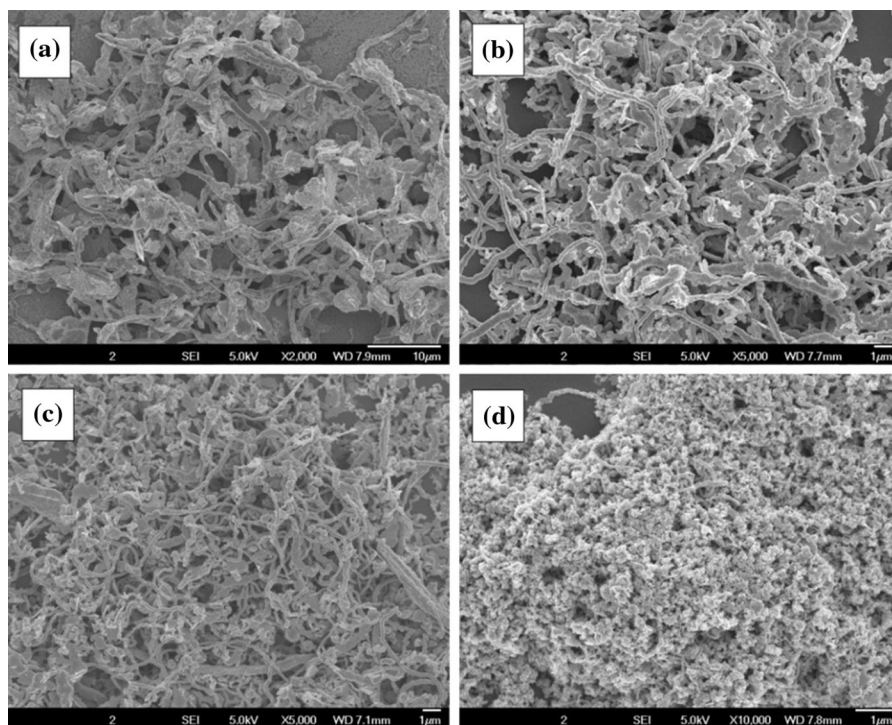


Fig. 3 SEM images of one-dimensional Au@PTh fibers; [Thiophene] = 5.0 mM [Thiophene]:[HAuCl₄] = **a** 1:1, **b** 2:1, **c** 3:1, **d** 5:1

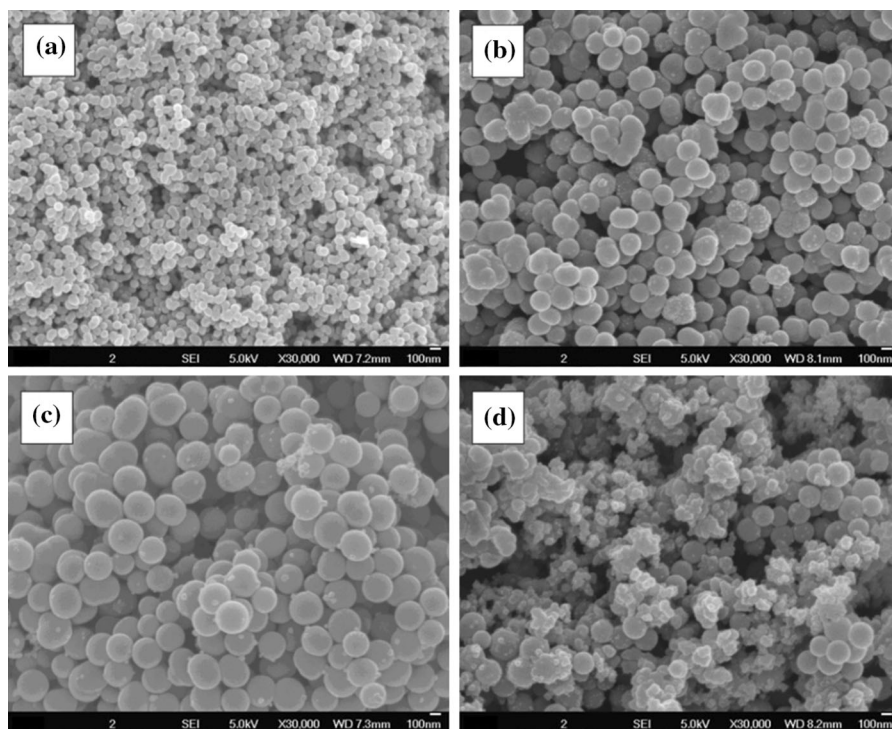


Fig. 4 SEM images of polythiophene nanostructures; [Thiophene] = 50 mM [Thiophene]:[HAuCl₄] = **a** 10:1, **b** 5:1, **c** 3:1, **d** 2:1

distinct PTh nanospheres with uniform size of ~ 191 nm (Fig. 4b) and ~ 272 nm (Fig. 4c) were formed, while smaller PTh nanospheres (~ 77 nm) were produced at the molar ratio of 10:1 (Fig. 4a). At a fixed concentration of thiophene, the dosage of HAuCl_4 determines the size of PTh nanospheres. The detailed size distributions of PTh nanospheres prepared at different thiophene/ HAuCl_4 molar ratios were shown in Fig. S3. On the other hand, at a higher thiophene/ HAuCl_4 molar ratio of 2:1 and 1:1, PTh nanosphere formation broke down and agglomerate particles were obtained. We postulate that the high concentration of HAuCl_4 results in a high reaction energy that disrupted the formation of PTh nanospheres.

Formation mechanism of PTh–Au nanocomposite

Based on the investigations mentioned above, a possible formation mechanism of PTh–Au composites is proposed as shown in Fig. 5. In the reaction system, monomer thiophene was polymerized by using HAuCl_4 as the oxidant, which is driven by simultaneous reduction of HAuCl_4 to gold nanostructures. When the thiophene concentration is extremely low (below 1.0 mM), the polymerization has a low conversion rate which results in the generation of thiophene oligomers (20 % yield). The resulting gold nanoparticles were capped by oligothiophene as a protective agent to form Au@PTh core–shell nanoparticles with different sizes. As the concentration of thiophene increasing to 1.0 mM, more thiophene oligomers will be produced (31 % yield). Thiophene oligomers adsorbed on the surfaces of gold nanoparticles prefer to aggregate and assemble which result in the formation of short stick-like Au@PTh nanostructures. With increasing monomer concentration to 5.0 mM, more and more stick-like Au@PTh nanostructures and Au@PTh nanoparticles tend to self-assemble and transform into one-dimensional Au@PTh fibers with different diameters (37 % yield) (Sajanlal et al. 2008). As a result, thiophene may not only work as a reductant but also play as a capping agent to guide the growth of the nanocables. All the Au@PTh composites obtained in different monomer concentrations have the same structures with AuNPs as the core and PTh as the shell. This analysis is supported by the gradual change of the UV–Vis–NIR absorption spectra. As the yield of the PTh increases,

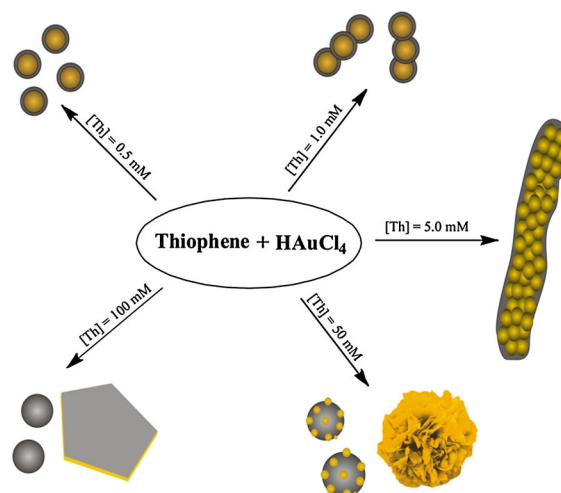


Fig. 5 Schematic illustration of the formation of PTh–Au composites prepared with various concentrations of thiophene

the UV absorption peak between 300 nm and 400 nm becomes more intense. The capping of AuNPs with increasing thickness of PTh shell makes the aggregated AuNPs show a broad absorption peak and gradually shift to near-infrared region.

At a high thiophene concentration of 50 mM, we postulate that most of the monomers form spherical nanodroplets prior to polymerization because of the low solubility of thiophene in water. The oxidative polymerization will take place inside nanosized thiophene monomer droplets as nanoreactors, dispersed in aqueous medium. The formation of thiophene nanodroplets in aqueous solution results in the exclusion of AuCl_4^- ions during the reaction. Consequently, part of the formed gold nanocrystals were incorporated on the periphery of the PTh nanospheres to form AuNPs-decorated PTh nanospheres, while the other part of gold nanocrystals self-assembled into flower-like gold microparticles composed of gold nanosheets (Figs. 2c, 1e). At a high enough concentration of thiophene, the amount of resulting PTh will be comparatively high (72 % yield). Enough polymers will be adsorbed prominently on the low index planes of the gold nanoparticles, which suppress the overall crystal growth, resulting in the formation of gold nanosheets and microsheets. Similar observations were reported by Bai et al. on the synthesis of poly(acrylic acid) (PAA)-based silver nanobelts, which were converted into nanoplates at higher concentrations of PAA (Bai

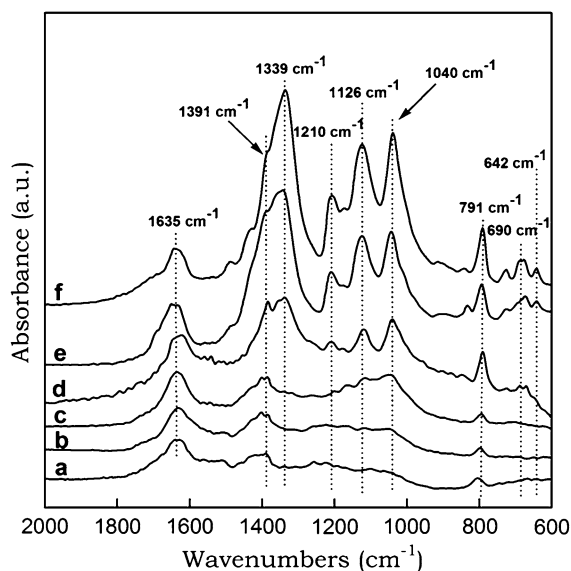


Fig. 6 FT-IR spectra of PTh-Au composites prepared with different thiophene concentrations: **a** 0.5 mM, **b** 1.0 mM, **c** 5.0 mM, **d** 10 mM, **e** 50 mM, **f** 100 mM. Other reaction conditions: [Thiophene]/[HAuCl₄] = 3:1, 25 °C, *t* = 24 h

et al. 2007). So, at a higher monomer concentration of 100 mM, except the formation of PTh nanospheres (75 % yield), these first-formed AuNPs recrystallized into large-sized gold microsheets by Ostwald ripening (Fig. 2d, h) (Chayer et al. 1997).

Chemical and electronic properties

The chemical and electronic structures of PTh-Au composites prepared with different thiophene concentrations at a fixed thiophene/HAuCl₄ molar ratio of 3:1 were studied by FT-IR and UV-Vis spectroscopies, respectively. The FT-IR spectra of Au@PTh core-shell nanoparticles, Au@PTh fibers, and AuNPs-decorated PTh nanospheres are shown in Fig. 6. The FT-IR spectra of Au@PTh nanoparticles and fibers exhibited weak absorbance peaks, which can be possibly due to the insignificant amount of polythiophene as compared with gold nanocrystals in the core-shell structures. As expected, the FT-IR spectra of AuNPs-decorated PTh nanospheres show typical bands of polythiophene. The sharp band around 791 cm⁻¹ is ascribed to C-H out-of-plane bending vibration characteristic of 2,5-disubstituted thiophene unit, indicating the α -position linkage between the

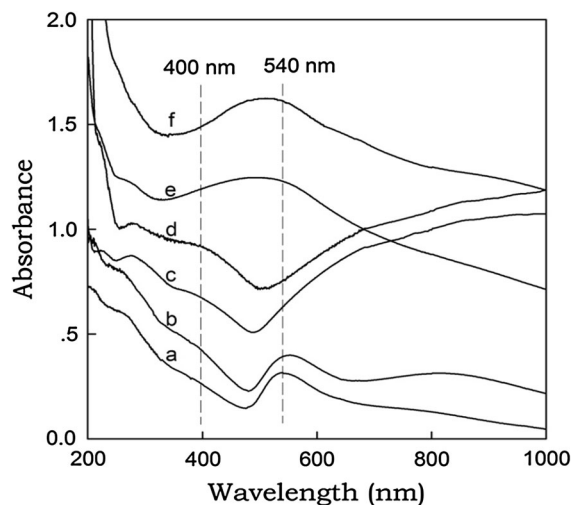


Fig. 7 UV-Vis-NIR absorption spectra of PTh-Au composites prepared with different thiophene concentrations: **a** 0.5 mM, **b** 1.0 mM, **c** 5.0 mM, **d** 10 mM, **e** 50 mM, **f** 100 mM. Other reaction conditions: [Thiophene]/[HAuCl₄] = 3:1, 25 °C, *t* = 24 h

thiophene rings. The four IR characteristic peaks at 1,339 cm⁻¹ (the stretching vibration of C _{β} -C _{β}), 1,210 cm⁻¹ (the stretching vibration of C _{α} -C _{α}), 1,126 cm⁻¹ (the in-plane bending of the aromatic C-H), and 1,040 cm⁻¹ (the in-plane stretching vibration of C-H) are observed, which are in good agreement with those of polythiophene (Fu et al. 2001; Cao et al. 1987). The peak at 1,392 cm⁻¹ originated from the bipolaron states of the doped PTh materials (Park et al. 2010). The characteristic peaks at 642 and 690 cm⁻¹ correspond to C-S bending and C-S-C ring symmetric deformation (Fig. 7).

The UV-Vis-NIR absorption spectra of PTh-Au composites show the morphology-/size-dependent optical properties (Fig. 7). The gold nanoparticles, 5–50 nm in size, show a sharp absorption band in the 520–530-nm regions due to the collective oscillation of conduction electrons in response to optical excitation (Henglein and Meisel 1998). Au@PTh core-shell nanoparticles prepared in low thiophene concentration show a typical surface plasmon resonance (SPR) band around 540 nm with a 10–20-nm red shift compared with that of the free AuNPs. This is because the tight binding of PTh on the surface of AuNPs affects the surface plasmon absorption band (Jung et al. 2010; Sun et al. 2010). Furthermore, the weak absorbance

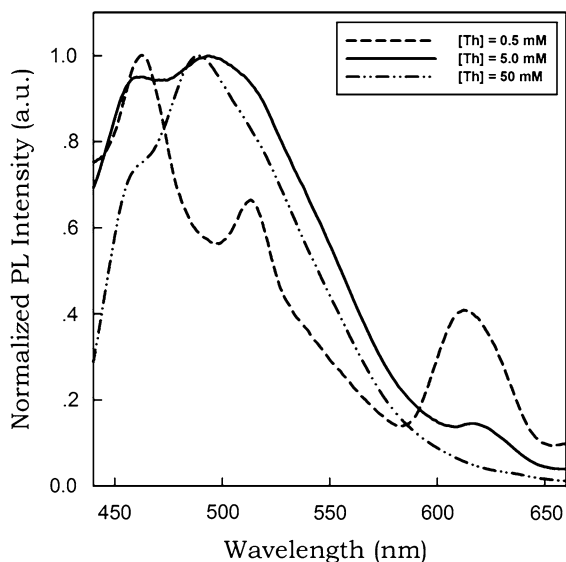


Fig. 8 Normalized photoemission spectra of three PTh–Au composites prepared with different thiophene concentrations at a fixed thiophene/HAuCl₄ molar ratio of 3:1, the excitation wavelength was fixed at 400 nm

peak of PTh at 400 nm is hard to be observed due to the small amount of PTh. However, the free AuNPs SPR band at 520–550 nm cannot be observed for one-dimensional Au@PTh nanofibers and microfibers. Instead, a broad band extended into the near-infrared region appears due to the longitudinal component of the SPR band of aggregated AuNPs fibers (Zotti et al. 2007). In addition, a new shoulder peak at 400 nm appears due to the π – π^* transition for large π -conjugation structure of polythiophene (Li et al. 2003). When the concentration of thiophene increases to 50 mM and above, the obtained AuNPs-decorated PTh nanospheres exhibit a broad absorption band between 400 and 600 nm, which is assigned to the synergistic effect of the absorptions of PTh nanospheres at 400 nm and gold nanoparticles at 520–550 nm.

We also compared the photoluminescent (PL) properties of PTh–Au composites prepared with different thiophene concentrations ranging from 0.5 to 50 mM at a fixed thiophene/HAuCl₄ molar ratio of 3:1. Figure 8 shows the three normalized photoemission spectra of Au@PTh core–shell nanoparticles, Au@PTh fibers, and AuNPs-decorated PTh nanospheres. When the PTh–Au composites were excited at 400 nm in pure water, the nanocomposites

comprising AuNPs and polythiophene exhibited two typical emission peaks at 460 nm and 498–513 nm, which is consistent with previous reports (Panda and Chattopadhyay 2007; Guan et al. 2008). Also, there is a third small emission peak at 610 nm for Au@PTh core–shell nanoparticles. The emission at 610 nm belongs to the existence of partial small-sized Au@PTh core–shell nanoparticles because AuNPs with size larger than ~ 2 nm are not likely to be luminescent (Lee et al. 2010a, b).

With increasing monomer concentration, the relative intensity of the emission peaks of the PTh–Au composites at 460 and 610 nm decreased. AuNPs with size larger than 15 nm show PL quenching behavior (Wilcoxon et al. 1998; Jung et al. 2010). The ‘raspberry-like’ PTh–gold nanoaggregates prepared by Kim et al. do not show quenching behavior because AuNPs are about 5 nm. The mechanism of energy transfer can be responsible for the fluorescence quenching of PTh by AuNPs when the emission spectrum of the composite materials and the absorption spectrum of AuNPs overlap. Therefore, the emission peak at 513 nm of Au@PTh core–shell nanoparticles is relatively weak. When Au@PTh fibers with larger sizes were obtained, the quenching behavior of Au is relatively weak. With increasing thiophene concentration to 50 mM, AuNPs-decorated PTh nanospheres exhibited the maximum PL emission peak at 498 nm, which can be explained by the different morphologies of PTh–Au composites and the quenching effects of AuNPs resulting in a transformation of the PL spectrum shape (Choi et al. 2004). PTh is a typical red-light-emitting material. However, PTh–Au composites with different morphology and composition prepared by varying the concentration of thiophene exhibited different emission colors from red to blue.

Conclusions

We have successfully synthesized AuNPs-modified PTh nanospheres, Au@PTh core–shell nanoparticles, and fibers via a facile one-pot synthesis process without the use of templates or structure-directing agent. The structures of PTh nanomaterials and PTh–Au composites are found to be determined by the molar ratio of monomer/oxidant (thiophene/HAuCl₄) as well as the concentration of thiophene in aqueous

medium. PTh–Au nanocomposites including Au@PTh core–shell nanoparticles and nanofibers have potential applications in the field of nanoelectronics. On the other hand, the high surface area-to-volume ratio of PTh nanospheres translates to greater sensitivity and faster response time when functionalized with moieties in sensor application. Moreover, the presence of AuNPs with different size can quench or enhance the PL properties of the PTh through the strong SP effect, which makes PTh–Au nanocomposites very attractive materials applicable in biological and electro-optical fields. This study on the formation of PTh nanomaterials and PTh–Au composites will serve to facilitate further research on conducting polymers and metal-incorporated conducting polymers in future technologies.

Acknowledgments This work was supported by grants from the National Natural Science Foundation of China (Grant No. 21073054), Natural Science Foundation of Henan Province (Grant No. 102300410180), the Natural Science Foundation of the Education Department of Henan Province (Grant No. 0001F01124) and the Foundation for University Young Key Teacher by Henan Province (Grant No. 2009GGJS-021). We also thank Prof. Goh Suat Hong at the National University of Singapore for his helpful discussion

References

- Alkan S, Cutler CA, Reynolds JR (2003) High quality electrochromic polythiophenes via $\text{BF}_3 \cdot \text{Et}_2\text{O}$ electropolymerization. *Adv Funct Mater* 13:331–336
- Andersson MR, Berggren M, Inganäs O, Gustafsson G, Gustafsson-Carlberg J, Selse D, Hjertberg T, Wennerström O (1995) Electroluminescence from substituted poly (thiophenes): from blue to near-infrared. *Macromolecules* 28:7525–7529
- Bai J, Qin Y, Jiang C, Qi L (2007) Polymer-controlled synthesis of silver nanobelts and hierarchical nanocolumns. *Chem Mater* 19:3367–3369
- Bai X, Zheng L, Li N, Dong B, Liu H (2008) Synthesis and characterization of microscale gold nanoplates using Langmuir monolayers of long-chain ionic liquid. *Cryst Growth Des* 8:3840–3846
- Bao Z, Lovinger AJ (1999) Soluble regioregular polythiophene derivatives as semiconducting materials for field-effect transistors. *Chem Mater* 11:2607–2612
- Bao Z, Dodabalapur A, Lovinger AJ (1996) Soluble and processable regioregular poly (3-hexylthiophene) for thin film field-effect transistor applications with high mobility. *Appl Phys Lett* 69:4108–4110
- Cao Y, Guo D, Pang M, Qian R (1987) Studies on iodine doped thiophene oligomers. *Synth Met* 18:189–194
- Chayer M, Faïd K, Leclerc M (1997) Highly conducting water-soluble polythiophene derivatives. *Chem Mater* 9:2902–2905
- Choi Y, Tepavcevic S, Xu Z, Hanley L (2004) Optical and chemical properties of polythiophene films produced via surface polymerization by ion-assisted deposition. *Chem Mater* 16:1924–1931
- Fu M, Zhu Y, Tan R, Shi G (2001) Aligned polythiophene micro-and nanotubules. *Adv Mater* 13:1874–1877
- Gevorgyan SA, Krebs FC (2008) Bulk heterojunctions based on native polythiophene. *Chem Mater* 20:4386–4390
- Gök A, Omastová M, Yavuz AG (2007) Synthesis and characterization of polythiophenes prepared in the presence of surfactants. *Synth Met* 157:23–29
- Guan H, Zhou P, Zhou X, He Z (2008) Sensitive and selective detection of aspartic acid and glutamic acid based on polythiophene–gold nanoparticles composite. *Talanta* 77:319–324
- Gunes S, Neugebauer H, Sariciftci NS (2007) Conjugated polymer-based organic solar cells. *Chem Rev* 107:1324–1338
- Guo Z, Zhang Y, Duanmu Y, Xu L, Xie S, Gu N (2006) Facile synthesis of micrometer-sized gold nanoplates through an aniline-assisted route in ethylene glycol solution. *Colloids Surf A* 278:33–38
- Henglein A, Meisel D (1998) Radiolytic control of the size of colloidal gold nanoparticles. *Langmuir* 14:7392–7396
- Ho H-A, Najari A, Leclerc M (2008) Optical detection of DNA and proteins with cationic polythiophenes. *Acc Chem Res* 41:168–178
- Jung YJ, Govindaiah P, Park T-J, Lee SJ, Kim JH, Cheong IW (2010) Luminescent gold–poly (thiophene) nanoaggregates prepared by one-step oxidative polymerization. *J Mater Chem* 20:9770–9774
- Kim Y, Cook S, Tuladhar SM, Choulis SA, Nelson J, Durrant JR, Bradley DD, Giles M, McCulloch I, Ha C-S (2006) A strong regioregularity effect in self-organizing conjugated polymer films and high-efficiency polythiophene: fullerene solar cells. *Nat Mater* 5:197–203
- Kim YS, Lee HJ, Govindaiah P, Son W, Koh W-G, Cheong IW, Kim JH (2014) Preparation of Fe_3O_4 -embedded poly(styrene)/poly(thiophene) core/shell nanoparticles and their hydrogel patterns for sensor applications. *Materials* 7:195–205
- Kline RJ, McGehee MD, Toney MF (2006) Highly oriented crystals at the buried interface in polythiophene thin-film transistors. *Nat Mater* 5:222–228
- Lee JM, Lee SJ, Jung YJ, Kim JH (2008a) Fabrication of nanostructured polythiophene nanoparticles in aqueous dispersion. *Curr Appl Phys* 8:659–663
- Lee SJ, Lee JM, Cheong IW, Lee H, Kim JH (2008b) A facile route of polythiophene nanoparticles via Fe^{3+} -catalyzed oxidative polymerization in aqueous medium. *J Polym Sci Part A Polym Chem* 46:2097–2107
- Lee SJ, Lee JM, Cho H-Z, Koh WG, Cheong IW, Kim JH (2010a) Poly (thiophene) nanoparticles prepared by Fe^{3+} -Catalyzed oxidative polymerization: a size-dependent effect on photoluminescence property. *Macromolecules* 43:2484–2489
- Lee C-W, Takagi C, Truong T, Chen Y-C, Ostafin A (2010b) A Luminescent Au nanoparticles with a pH-responsive

- nanoparticle-supported molecular brush. *J Phys Chem C* 114:12459–12468
- Li G, Bhosale S, Wang T, Zhang Y, Zhu H, Fuhrhop JH (2003) Gram-scale synthesis of submicrometer-long polythiophene wires in mesoporous silica matrices. *Angew Chem Int Ed* 42:3818–3821
- Li XG, Li J, Huang MR (2009a) Facile optimal synthesis of inherently electroconductive polythiophene nanoparticles. *Chem Eur J* 15:6446–6455
- Li X-G, Li J, Meng Q-K, Huang M-R (2009b) Interfacial synthesis and widely controllable conductivity of polythiophene microparticles. *J Phys Chem B* 113:9718–9727
- Mallick K, Witcomb MJ, Scurrrell MS (2007) Directional assembly of polyaniline functionalized gold nanoparticles. *J Phys Condens Matter* 19:196225
- McCullough RD (1999) The chemistry of conducting polythiophenes. *Adv Mater* 10:93–116
- McCullough RD, Lowe RD, Jayaraman M, Anderson DL (1993) Design, synthesis, and control of conducting polymer architectures: structurally homogeneous poly (3-alkylthiophenes). *J Org Chem* 58:904–912
- Mwaura JK, Zhao X, Jiang H, Schanze KS, Reynolds JR (2006) Spectral broadening in nanocrystalline TiO₂ solar cells based on poly (p-phenylene ethynylene) and polythiophene sensitizers. *Chem Mater* 18:6109–6111
- Nicholson PG, Ruiz V, Macpherson JV, Unwin PR (2005) Enhanced visible photoluminescence in ultrathin poly (3-hexylthiophene) films by incorporation of Au nanoparticles. *Chem Commun* 8:1052–1054
- Ogawa K, Stafford JA, Rothstein SD, Tallman DE, Rasmussen SC (2005) Nitrogen-functionalized polythiophenes: potential routes to new low band gap materials. *Synth Met* 152:137–140
- Panda BR, Chattopadhyay A (2007) A water-soluble polythiophene–Au nanoparticle composite for pH sensing. *J Colloid Interface Sci* 316:962–967
- Panda BR, Singh AK, Ramesh A, Chattopadhyay A (2008) A rapid estimation of bacteria by a fluorescent gold nanoparticle– polythiophene composite. *Langmuir* 24:11995–12000
- Pandey P, Arya SK, Matharu Z, Singh SP, Datta M, Malhotra BD (2008) Polythiophene gold nanoparticles composite film for application to glucose sensor. *J Appl Polym Sci* 110:988–994
- Park DH, Hong YK, Kim MS, Cho EH, Choi WJ, Kim KH, Park Q, Kim D-C, Song H, Kim J (2010) Nanoscale photoluminescence of light-emitting poly (3-methylthiophene) nanotubes hybridized with Au nanoparticles. *Synth Met* 160:604–608
- Sajanlal P, Sreeprasad T, Nair AS, Pradeep T (2008) Wires, plates, flowers, needles, and core-shells: diverse nanostructures of gold using polyaniline templates. *Langmuir* 24:4607–4614
- Sheina EE, Khersonsky SM, Jones EG, McCullough RD (2005) Highly conductive, regioregular alkoxy-functionalized polythiophenes: a new class of stable, low band gap materials. *Chem Mater* 17:3317–3319
- Skotheim TA, Elsenbaumer RL, Reynolds JR (1998) *Handbook of Conducting Polymers*, 2nd edn. Marcel Dekker, New York
- Sun S, Salim T, Wong LH, Foo YL, Boey F, Lam YM (2010) A new insight into controlling poly (3-hexylthiophene) nanofiber growth through a mixed-solvent approach for organic photovoltaics applications. *J Mater Chem* 21:377–386
- Sun H, He J, Xing S, Zhu L, Wong YJ, Wang Y, Zhai H, Chen H (2011) One-step synthesis of composite vesicles: direct polymerization and in situ over-oxidation of thiophene. *Chem Sci* 2:2109–2114
- Suzuki K, Zhang H, Saito K, Garitaonandia J, Goikolea E, Insausti M (2011) Ferromagnetism of polythiophene-capped Au nanoparticles. *J Appl Phys* 109:07E328
- Thompson BC, Fréchet JM (2008) Polymer–fullerene composite solar cells. *Angew Chem Int Ed* 47:58–77
- Tran HD, Wang Y, D'Arcy JM, Kaner RB (2008) Toward an understanding of the formation of conducting polymer nanofibers. *ACS Nano* 2:1841–1848
- Wang Z, Wang Y, Xu D, S-W Kong E, Zhang Y (2010) Facile synthesis of dispersible spherical polythiophene nanoparticles by copper (II) catalyzed oxidative polymerization in aqueous medium. *Synth Met* 160:921–926
- Wilcoxon JP, Martin JE, Parsapour F, Wiedenman B, Kelley DF (1998) Photoluminescence from nanosize gold clusters. *J Chem Phys* 108:9137–9143
- Zotti G, Vercelli B, Battagliarin M, Berlin A, Hernandez V, Navarrete JL (2007) Oligothiophene-and oligopyrrole-mediated aggregation of gold nanoparticles. *J Phys Chem C* 111:5886–5892
- Zou Y, Wu W, Sang G, Yang Y, Liu Y, Li Y (2007) Polythiophene derivative with phenothiazine-vinylene conjugated side chain: synthesis and its application in field-effect transistors. *Macromolecules* 40:7231–7237